Lipid binding and membrane penetration of polymyxin B derivatives studied in a biomimetic vesicle system

Marina KATZ*, Haim TSUBERY†, Sofiya KOLUSHEVA*, Alex SHAMES*, Mati FRIDKIN† and Raz JELINEK*[1]

*Department of Chemistry and Staedler Minerva Center for Mesoscopic Macromolecular Engineering, Ben Gurion University of the Negev, Beersheva 84105, Israel, and †Department of Organic Chemistry, Weizmann Institute of Science, Rehovot 76100, Israel

Understanding membrane interactions and cell-wall permeation of Gram-negative bacteria is of great importance, owing to increasing bacterial resistance to existing drugs and therapeutic treatments. Here we use biomimetic lipid vesicles to analyse membrane association and penetration by synthetic derivatives of polymyxin B (PMB), a potent naturally occurring antibacterial cyclic peptide. The PMB analogues studied were PMB nonapeptide (PMBN), in which the hydrophobic alkyl residue was cleaved, PMBN diastereomer containing D- instead of L-amino acids within the cyclic ring (dPMBN) and PMBN where the hydrophobic alkyl chain was replaced with an Ala_6 repeat (Ala_6-PMBN). Peptide binding measurements, colorimetric transitions induced within the vesicles, fluorescence quenching experiments and ESR spectroscopy were applied to investigate the structural parameters underlying the different membrane-permeation pro-files and biological activities of the analogues. The experiments point to the role of negatively charged lipids in membrane binding and confirm the prominence of lipopolisaccharide (LPS) in promoting membrane association and penetration by the peptides. Examination of the lipid interactions of the PMB derivatives shows that the cyclic moiety of PMB is not only implicated in lipid attachment and LPS binding, but also affects penetration into the inner bilayer core. The addition of the Ala_6 peptide moiety, however, does not significantly promote peptide insertion into the hydrophobic lipid environment. The data also indicate that the extent of penetration into the lipid bilayer is not related to the overall affinity of the peptides to the membrane.

Key words: antibacterial peptides, fluorescence quenching, membranes, polydiacetylene, polymyxin B.

INTRODUCTION

The emergence of bacterial strains resistant to conventional antibiotics is a major cause for inefficient therapy and increased mortality from bacterial infection. These phenomena have led to intensive efforts aimed at the development of novel drugs targeting the bacterial cell membranes. Gram-negative bacteria, such as *Escherichia coli*, have two cell-envelope membranes. The inner cytoplasmic membrane consists primarily of phospholipids, whereas the outer membrane is an asymmetric membrane composed mainly of lipopolysaccharide (LPS) in the outer monolayer, and phospholipids (with a composition similar to that of the cytoplasmic membrane) in its inner monolayer [1,2]. LPS plays a major role in conferring resistance of Gram-negative bacteria toward toxic agents, most likely by participating in the formation of an effective permeability barrier at the outer membrane. Several hypotheses have been presented to explain the unique permeability properties of LPS, utilizing various structural differences between LPS and phospholipids. Existing models variably identify the biological determinants of LPS in its hydrophobic core [3], head-groups [4] or other factors.

Polymyxin B (PMB), a cyclic cationic antibiotic decapeptide (Figure 1A), has been one of the most efficient compounds exhibiting LPS binding and outer-membrane-disorganizing capabilities [5]. Specifically, PMB is believed to inhibit the biological activities of LPS through high-affinity binding to the lipid A moiety [6]. The therapeutic applications of PMB are limited, however, because of its high toxicity. Previous studies have attempted to overcome PMB toxicity through various chemical modifications [7–9]. Polymyxin B nonapeptide (PMBN), for example, is a cyclic peptide obtained from PMB by proteolytic cleavage of its N-terminal hydrophobic acyl residue (Figure 1A) with enzymes such as papain or ficin [10]. PMBN, however, is a poor antimicrobial compound, but still capable of binding, like PMB, to LPS, rendering Gram-negative bacteria susceptible to various hydrophobic antibiotics by synergistic processes [11].

Other PMB and PMBN derivatives have been synthesized and their biological properties investigated [12–14]. Table 1 summarizes the sequences and membrane sensitization of PMB and its derivatives studied here. The analogues were constructed through modifications of the cyclic ring or the hydrophobic N-terminal residue of the peptide. These compounds include PMBN, dPMBN (PMBN containing diastereomeric D- rather than L-amino acid residues) constructed to probe chirality and structural effects within the cyclic ring [13], and Ala_6-PMB (PMBN with an Ala_6 residue covalently attached; Figure 1B) synthesized in order to examine the effects of a mildly hydrophobic peptidic sequence [14]. Previous studies have detected distinct differences in the biological properties and membrane permeation of those peptides (Table 1), although all have insignificant antibacterial activities compared with PMB [12–14].

In the present study we analysed lipid binding and membrane penetration of the PMBN derivatives. Molecular and structural information on membrane interactions of the PMBN derivatives have been obtained here through application of a newly developed biomimetic lipid/polydiacetylene (PDA) membrane assay [15–17]. The lipid/PDA platform consists of vesicles composed of interspersed natural lipids and polymerized PDA, which undergo
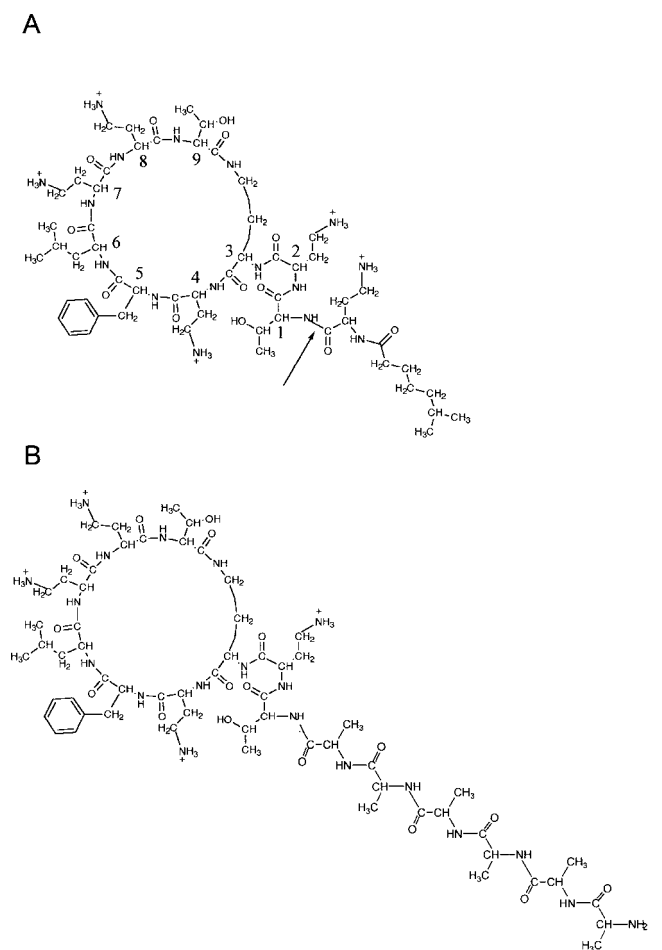
A

B

Figure 1   (A) Structure of PMB (arrow indicating the cleavage site yielding PMBN) and (B) structure of Ala$_6$-PMBN

Table 1   Sequences and sensitizing activities of PMB, PMBN and the PMBN analogues

Peptide	Sequence*	Relative OM permeability†
PMB	6-Methylheptanoyl/octanoyl-XTXcyclo[XX**F**LXXT]	‡
Ala$_6$-PMBN	AAAAAATXcyclo-[XX**F**LXXT]	++++
PMBN	TXcyclo[XX**F**LXXT]	++++++
dPMBN	**TX**cyclo[**XXF**L**XX**T]	+

* D-Amino acids are in **boldface** text; X is diaminobutyric acid.

† Outer membrane (OM) permeability is the peptide's ability to increase the penetration of a hydrophobic antibiotic through the OM of *E.coli* and *Klebsiella pneumoniae* detailed in [12–14], where ++++++ represents the highest activity.

‡ PMB has a direct high antibacterial activity [MIC (minimum inhibitory concentration) 3–4 μg/ml], whereas the other analogues lack such activity.

rapid blue-to-red transitions induced by interactions with varied biological molecules. Previous studies of the biophysical properties of lipid/PDA vesicles indicate that the lipids and PDA form interspersed interacting microscopic phases [18–21]. Importantly, the phospholipids incorporated within the PDA matrix adopt a bilayer structure, the dominant lipid organization within cellular membranes [21]. Published data further point to the contribution

of changes in fluidity within the lipid domains for induction of the blue-to-red transitions [15,21].

We have previously demonstrated that PDA-based vesicles could be used for studying membrane processes such as peptide–membrane interactions [15,16,22], membrane permeation by penetration enhancers [18] and biological recognition events occurring at membrane interfaces [17]. Of particular importance in the context of the present study, the polymeric PDA matrix which forms the scaffold of the mixed vesicles can incorporate different lipid components while maintaining its overall sensitivity to membrane properties and processes [21,22]. In the present study, application of lipid binding measurements, colorimetric analysis and spectroscopic techniques such as fluorescence quenching and ESR sheds light on membrane interactions of the PMB derivatives and their permeation properties.

EXPERIMENTAL

Materials

Phospholipids, including dimyristoyl phosphatidylcholine (DMPC), dimyristoyl phosphatidylglycerol (DMPG) and LPS from *E. coli* 055:B5 were purchased from Sigma. LPS was dialysed in 1 mM EDTA (Sigma) for 24 h, followed by distilled water, in order to remove excess bivalent cations (which generally cause precipitation of lipid/PDA vesicles). The diacetylenic monomer 10,12-tricosadiynoic acid was purchased from GFS Chemicals (Powell, OH, U.S.A.), washed in chloroform, and filtered through a 0.45-μm-pore-size filter prior to use.

PMB sulphate was purchased from Sigma. Synthesis and purification of the PMB derivatives is described elsewhere [12–14]. The more abundant alamethicin homologue containing glutamic acid at position 18 (Aib-Pro-Aib-Ala-Aib-Ala-Gln-Aib-Val-Aib-Gly-Leu-Aib-Pro-Val-Aib-Aib-Glu-Gln-Phe-OH, where Aib denotes α-aminoisobutyric acid) was used (Sigma).

Vesicle preparation

Preparation of vesicles containing lipid components and PDA (DMPG/DMPC/PDA, 1:1:3 molar ratio; LPS/DMPC/PDA, 0.2:2:3 molar ratio) was carried out as follows. All lipid constituents were dissolved in chloroform/ethanol (1:1,v/v) and dried together *in vacuo* up to constant weight, followed by addition of deionized water and probe sonication (Ultrasonic model XL2020 sonicator; Misonix Inc., Farmingdale, NY, U.S.A.; output power 550 W) at 70 °C for 2–3 min. The vesicle solution was then cooled at room temperature and was kept at 4 °C overnight. The vesicles were then polymerized using irradiation at 254 nm for 10–20 s, with the resulting solutions exhibiting an intense blue appearance.

Dansyl-PMBN displacement assay

The fluorescence of dansyl-PMBN bound to vesicles was measured at 28 °C using an SLM Aminco–Bowman spectrofluorimeter with excitation at 340 nm and emission acquired at 485 nm. Increasing quantities of dansyl-PMBN (1×10^{-5}–1×10^{-3} M) were added to a quartz cuvette containing vesicle solution (7.5 μl, 1 mM) and buffer (7.5 μl, Tris base, 50 mM, pH 8). The solution was diluted to 1 ml with distilled water and fluorescence was recorded. The fluorescence of vesicle-bound dansyl-PMBN (1×10^{-4} M) was determined at 85 % of maximum fluorescence, which served as the control sample. The decrease in dansyl-PMBN

fluorescence (percentage decrease from control) as a result of progressive addition of peptides was then measured.

Determination of partition coefficients

Calibration graphs for determination of concentrations of the soluble peptides were initially constructed using the Lowry method [23]. The calibration graphs were employed to evaluate the concentrations of peptides unbound to the lipid/PDA vesicles. Increasing quantities of peptide were added to aqueous lipid/PDA vesicle solutions (0.5 mM total lipid concentration; with 25 mM Tris buffer at pH 8), the solutions were left at room temperature for a few minutes to allow equilibration, and were centrifuged at 85 000 g for 40 min in order to precipitate the vesicle–peptide aggregates. The concentration of soluble (unbound) peptide in the supernatant was determined from the calibration curve, and was subtracted from the initial concentration to yield the amount of bound peptide.

UV-vis (UV–visible) measurements

Samples were prepared by adding peptides (at final concentrations of between 5 and 100 μM) to 0.06 ml of vesicle solution at 0.5 mM total lipid concentration and 25 mM Tris (pH 8). The PMBN derivatives were dissolved in water (in the synergy experiments alamethicin was dissolved in trifluoroethanol). Following addition of the peptides, the solutions were diluted to 1 ml and UV-vis spectra were acquired. UV-vis spectroscopy measurements were carried out at 28 °C on a Jasco V-550 spectrophotometer, using a 1-cm-optical-pathlength cell.

A quantitative value for the extent of the blue-to-red colour transitions within the vesicle solutions is given by the colorimetric response (%CR), which is defined as follows [24]:

$$\%CR = [(PB_0 - PB_1)/PB_0] \times 100$$

where $PB = A_{blue}/(A_{blue} + A_{red})$, A is the absorbance either at the 'blue' component in the UV-vis spectrum (640 nm) or at the 'red' component (500 nm) (note that 'blue' and 'red' refer to the visual appearance of the material, not its actual absorbance). PB_0 is the blue/red ratio of the control sample (before induction of a colour change) and PB_1 is the value obtained for the vesicle solution after colorimetric transition occurs.

Fluorescence quenching measurements

The fluorescent probe NBD-PE [N-(7-nitrobenz-2-oxa-1,3-diazol-4-yl)-1,2-dihexadecanoyl-sn-glycero-3-phosphoethanolamine) triethylammonium salt was purchased from Molecular Probes, Inc. (Eugene, OR, U.S.A.). NBD-PE was dissolved in chloroform, added to phospholipids at 1 mol % and dried together *in vacuo* before sonication (see under the subsection 'Vesicle preparation'). Addition of NBD-labelled lipids did not affect either the blue colour of the vesicles or the blue-to-red transitions.

Samples were prepared by adding peptides, at a concentration of 15 μM, bound to 0.06 ml of vesicle solution and at 0.5 mM total lipid concentration, to 25 mM Tris base, pH 8. The quenching reaction was initiated by adding sodium dithionite ($Na_2S_4O_2$; Aldrich) from a 0.6 M stock solution, prepared in 50 mM Tris base buffer, pH 11, to a final concentration of 10 mM. The decrease in fluorescence was recorded for 120 s at 28 °C using 467 nm excitation and 535 nm emission on an Edinburgh Co. (Edinburgh, Scotland, U.K.) FL920 spectrofluorimeter. The fluorescence decay was calculated as a percentage of the initial fluorescence measured before the addition of dithionite.

ESR

Samples for the ESR experiments were prepared using the spin label 5-doxyl stearic acid (5-DS, Sigma). 5-DS was added to the vesicle samples after the polymerization step at a spin label/lipid molar ratio of 1:100. Samples were placed in a 20-mm-long, 1-mm-internal-diameter quartz capillary and recorded using a Bruker EMX-220 digital X-band spectrometer operating at room temperature. The amplitudes of 12.5 and 100 kHz modulation and the microwave power level were chosen at subcritical values (0.5 G and 10 mW respectively) to reach the best signal-to-noise ratio. Processing of the ESR spectra (digital filtering, double integration, etc.) was carried out using Bruker WIN-EPR software.

RESULTS

Membrane interactions of PMB and PMBN: synergy experiments

An important biological characteristic of both PMB and its PMBN derivative is the facilitation of membrane penetration for varied chemical and biological molecules through synergistic effects [12–14]. The penetration synergy has been ascribed to the strong interactions of the peptides with the LPS head-groups, thus reducing the permeation barrier of bacterial outer membranes [25–27]. We have examined whether synergy effects are also observed for PMB and PMBN interactions with the biomimetic LPS/DMPC/PDA chromatic vesicles (Figure 2). We chose to examine the synergy effects specifically only for PMB, the parent molecule, and PMBN, the generic derivative, for which biological synergies were previously determined [26,27].

The initial blue colour of the vesicles (%CR defined as zero) arises from the electronic delocalization within the conjugated PDA backbone [28]. Furthermore, the blue-to-red transitions (corresponding to an increased %CR) observed in PDA systems have been ascribed to structural alterations of the conjugated network [28,29]. Previous studies have indicated that the lipid moieties form organized bilayer domains within the lipid/PDA vesicles. It was also shown that interactions between the lipid domains and membrane-active compounds induce colour transitions by perturbation of the polymer pendant side chains through the molecular interface between the lipids and the PDA matrix [15,16,21]. The lipid compositions of the vesicles employed in the present study were designed to create model systems representing bacterial membranes, in particular for studying the role and significance of LPS at the outer bacterial wall (in the case of LPS/DMPC/PDA) for peptide binding and permeation.

Figure 2 depicts the colorimetric transitions (%CR; see the Experimental section) induced by PMB and PMBN added *in trans* with the hydrophobic membrane peptide alamethicin [30] to aqueous solutions containing LPS/DMPC/PDA vesicles. The blue-to-red colour changes depend upon the concentration of the peptide in the vesicle solution, as shown in Figure 2. We have previously shown that alamethicin, a short transmembrane antibacterial peptide, induces moderate colorimetric transitions when added to aqueous solutions containing DMPC/PDA vesicles [15]. The curves presented in Figure 2 indicate that the %CR increased at higher concentrations of alamethicin in the LPS/DMPC/PDA vesicle solutions (corresponding to more pronounced blue-to-red transitions). However, the colorimetric graphs specifically demonstrate that, when PMB (Figure 2A) or PMBN (Figure 2B) are added with alamethicin *in trans*, greater blue-to-red transitions are induced compared with the addition of alamethicin alone. For example, at a concentration of 150 μM, alamethicin induced a %CR of 80 % in the presence of PMB,
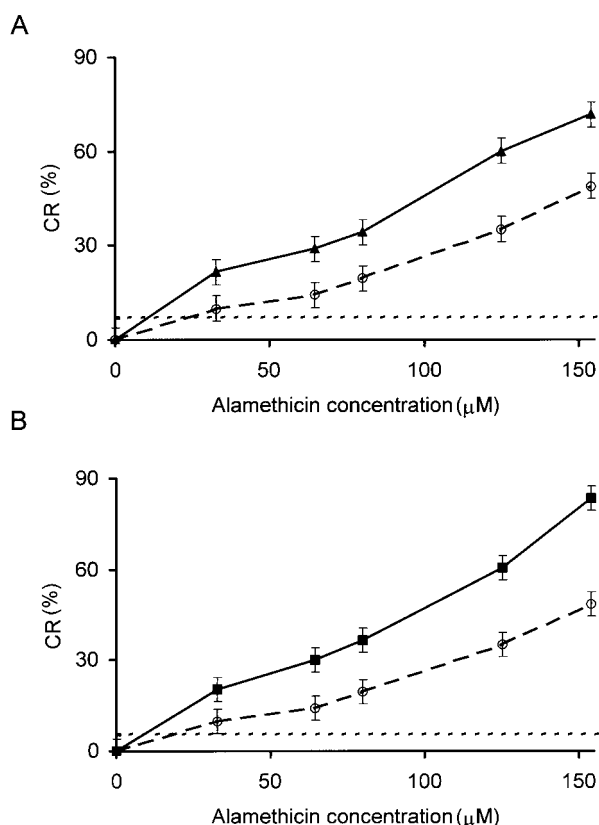
A

B

Figure 2 Synergy action observed for PMB and PMBN interacting with biomimetic lipid/PDA vesicles

Curves showing the relationship between the %CR and concentrations of PMB (**A**) or PMBN (**B**) in solutions containing LPS/DMPC/PDA vesicles to which were added alamethicin (------) or PMB (or PMBN) + alamethicin *in trans* (PMB or PMBN concentration kept constant at 2 μM) (---). The broken lines parallel with the *x*-axes indicate the %CR induced following addition of only PMB (or PMBN) at 2 μM concentration.

but only around 50 % without PMB (Figure 2A). Similarly, when PMBN and alamethicin are added *in trans* to the vesicles the induced %CR was 70 % (Figure 2B).

The effect of the peptides is clearly synergistic rather than additive – the parallel lines depicted in Figures 2(A) and 2(B) (at around 6 % CR) correspond to the %CR induced *only* by the constant PMB (or PMBN) concentrations added to the alamethicin solutions. Thus the higher %CR values recorded when ala-methicin is added to the vesicles in the presence of PMB or PMBN are not due to the simple sums of the individual %CR induced by alamethicin alone *and* PMB (or PMBN) alone – but are rather due to synergistic effects. Overall, the experiments depicted in Figure 2 verify the biological relevance of the colorimetric assay. The synergy apparent in the lipid/PDA vesicle system (Figure 2) is consistent with biological observations for both PMB and PMBN in conjunction with hydrophobic antibiotics [25–27].

Peptide-vesicle binding analysis

An essential element in the analysis of peptide–membrane in-teractions is evaluation of the relative binding of the peptides to the lipid bilayers. In order to explore the affinities of the PMBN derivatives to the vesicles, we carried out fluorescence experiments utilizing a dansyl-PMBN displacement assay [12,31] (Figure 3). This assay estimates the relative affinities of peptides to
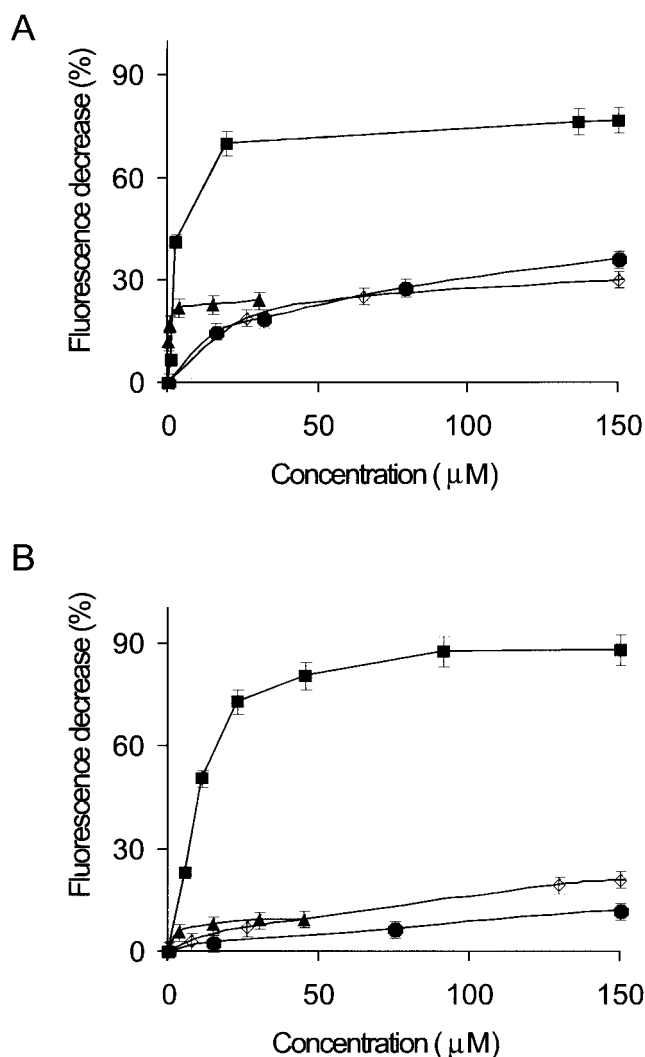
A

B

Figure 3 Dansyl-PMBN displacement assay

The Figure shows the decrease in fluorescence following displacement of dansyl-PMBN residues by the peptides; different extents of peptide affinity to lipid/PDA vesicles among PMB and the PMBN analogues are evident. Graphs depict the results of the dansyl-NPMB displacement assay (see the Experimental section). Peptides were added to solutions of (**A**) DMPG/DMPC/PDA vesicles or (**B**) LPS/DMPC/PDA vesicles. Peptides added: ■, PMB; ▲, dPMBN; ◇, Ala$_6$-PMBN; ●, PMBN.

lipid vesicles through their capabilities to displace lipid-associated dansyl-PMBN residues [12,31]. The dansyl group fluoresces when located within a hydrophobic lipid environment, whereas it undergoes self-quenching in aqueous solution following dis-placement by membrane-bound species [31]. The aim of the application of the dansyl-PMBN displacement assay in the lipid/ PDA vesicle system was to provide insight into differences in the binding profiles of the peptides and the concentration of putative binding sites for the peptides within the lipid moieties.

Figure 3 depicts the results of the displacement assay for DMPG/DMPC/PDA (Figure 3A) and LPS/DMPC/PDA vesicles (Figure 3B). Examination of the fluorescence quenching curves in Figure 3 reveals distinct differences among the binding profiles of the peptides. PMB exhibits the strongest binding in the two vesicle systems – apparent as both the fastest decrease in fluorescence (in relation to peptide concentration), as well as the maximal fluorescence inhibition achieved (the plateau in the inhibition
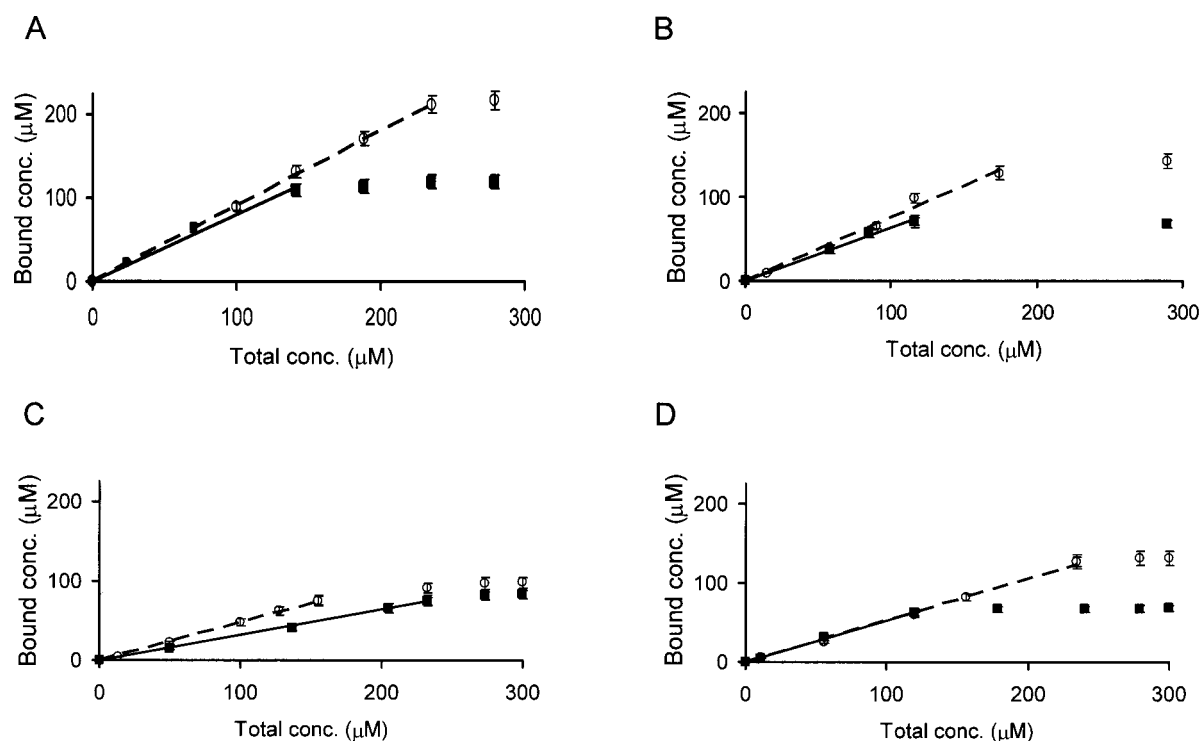
Figure 4   Centrifugation binding assay

Different partition coefficients and maximal bound concentrations are observed for the PMB analogues. Results are shown for DMPG/DMPC/PDA (■) and LPS/DMPC/PDA (○) vesicles. The lines correspond to the calculated slopes reflecting the partition coefficients of the peptides (see the text). Peptides: (**A**) PMB; (**B**) PMBN; (**C**) dPMBN; (**D**) Ala$_6$-PMBN.

curve). This result indicates that PMB replaces most of the lipid-bound dansyl-PMBN, leading to significantly higher quenching of the fluorescence of the dansyl moiety compared with the other analogues.

The dansyl-PMBN displacement assay (Figure 3) further indicates that the PMBN derivatives exhibit smaller affinities to the lipid/PDA vesicles compared with PMB. Differences are observed, however, in the binding properties *among* the peptides, and also in the relative binding of each peptide to a particular vesicle composition. dPMBN induces a steep rise in fluorescence inhibition in DMPG/DMPC/PDA and LPS/DMPC/PDA vesicles, suggesting high affinity of the peptide to the lipid moieties. However, the low plateaux reached at higher concentrations of dPMBN in both vesicle systems (20 % in DMPG/DMPC/PDA and about 10 % in the LPS-containing vesicles) indicate a relatively low displacement of dansyl-PMBN by the peptide. This result could be explained by localization of the diasteromeric peptide only at the lipid/water interface. The moderate slopes of fluorescence inhibition and low plateaux (under 30 % fluorescence inhibition) recorded in the cases of PMBN and Ala$_6$-PMBN indicate small substitution of the dansyl-PMBN by these analogues and low affinities to the vesicles.

The dansyl-PMBN assay provides useful information on the relative binding of the peptides to the lipid/PDA vesicles. We have further applied a centrifugation binding assay for evaluation of the water/vesicle partition coefficients of the peptides in the lipid/PDA system (Figure 4). The centrifugation binding assay determines the equilibrium concentration of the bound peptides by precipitation of the peptide–vesicles assemblies using ultra-centrifugation (see the Experimental section). Application of the centrifugation binding assay for determination of the binding profiles of the peptides is particularly important here because it

Table 2   Partition coefficients (fraction of vesicle-bound peptide concentrations) calculated for PMB and PMBN analogues with different vesicle compositions using the centrifugation binding assay (see the Experimental section)

Peptide	Vesicle composition . . .	Partition coefficient	
		LPS/DMPC/PDA	DMPG/DMPC/PDA
PMB		0.91	0.80
PMBN		0.76	0.63
dPMBN		0.48	0.33
Ala$_6$-PMBN		0.53	0.52

is a *direct* method for evaluation of peptide affinities, whereas the dansyl-PMBN displacement assay provides an *indirect* information upon the binding (based upon the fluorescence from the displaced dansyl-PMBN). Furthermore, the structural similarity between the PMBN analogues studied here and the dansyl-PMBN utilized in the displacement assay might affect the accurate comparison of relative peptide affinities using only the dansyl-PMBN fluorescence analysis.

Figure 4 depicts the results of the centrifugation binding assay applied for each peptide with DMPG/DMPC/PDA and LPS/DMPC/PDA vesicles respectively. Generally the binding curves consist of two domains: an almost-linear increase correlating the total peptide concentration and vesicle-bound concentration (with the slopes reflecting the water/lipid partition coefficients of the peptides; Table 2), followed by a plateau corresponding to the *maximal* concentration of vesicle-bound peptide (the binding capacity).

The results shown in Figure 4 and Table 2 reveal distinct differences in the binding profiles of the peptides. PMB exhibits a stoichiometric ratio closer to unity between bound and total peptide concentrations (Figure 4A and Table 2), which indicates the highest affinity among all peptides to the two vesicle models, similar to the results of the dansyl-PMBN displacement assay discussed above (Figure 3). In addition, the binding curves of PMB in Figure 4(A) show a greater maximal bound concentration of the parent peptide to the LPS/DMPC/PDA vesicles (approx. 225 μM compared with 120 μM for DMPG/DMPC/PDA), indicating higher binding capacity of PMB when LPS is incorporated within the vesicles. This observation attests to the significance of LPS in inducing PMB binding to bacterial outer membranes [31].

PMBN (Figure 4B) and its diastereomeric analogue dPMBN (Figure 4C) exhibit similarly higher binding capacities in LPS/DMPC/PDA vesicles compared with DMPG/DMPC/PDA vesicles, although to a lesser extent than PMB; maximal bound concentrations are about 140 and 100 μM for PMBN and dPMBN respectively (Figures 4B–4C). The partition coefficients of PMBN and dPMBN similarly indicate higher affinities of these peptides to vesicles containing LPS compared with DMPG (0.76 versus 0.63 for PMBN, 0.48 versus 0.33 for dPMBN; Table 2). However, the partition coefficients recorded for those analogues are again significantly lower than for PMB (Table 2), indicating lesser affinities of PMBN and dPMBN to the lipid bilayers and consistent with the lower biological activities of the analogues in relation to PMB (Table 1). Interestingly, Ala$_6$-PMBN (Figure 4D) seems to bind with almost identical affinities of about 0.5 to both vesicle compositions. This result suggests that the peptidic side chain is also affecting the binding of the Ala$_6$-PMBN analogue to the LPS-containing bacterial outer membrane.

Specific differences are observed, however, between the apparent binding strengths of the PMBN analogues to the LPS/DMPC/PDA vesicles compared with DMPG/DMPC/PDA vesicles, as extracted from the two binding assays (Figures 3 and 4). The centrifugation assay, for example, indicates higher affinities of the analogues to the LPS-containing vesicles (Figure 4), whereas the dansyl-PMBN assay seems to suggest more pronounced attachment to the DMPG/DMPC/PDA assemblies. It is important to emphasize that the PMBN moiety in the dansyl-PMB probe binds much more tightly to the LPS groups within the LPS/DMPC/PDA vesicles; thus its displacement by the PMBN analogues becomes much more 'costly' compared with the situation in the DMPG/DMPC/PDA vesicles. This is a primary reason for application of the centrifugation binding assay in the present study.

Colorimetric analysis of peptide–membrane interactions

The binding data presented in Figures 3 and 4 provide important information on the relative affinities of PMB and the PMB derivatives for membranes. The biological activities of the compounds are determined, however, not only by their binding properties, but to a large extent by the effects on membrane structure and organization [32]. Relative penetration and lipid bilayer disruption by the PMBN derivatives have been evaluated here through analysis of the colorimetric transitions induced within DMPG/DMPC/PDA vesicles and LPS/DMPC/PDA vesicles (Figure 5). Previous studies have indicated that lipid/PDA vesicles mimic cellular membrane environments and provide information on membrane processes [15,16]. We have shown that the lipid moieties in the mixed vesicles form organized bilayer domains within the polymer matrix [20,21], and that the blue-to-red transformations in lipid/PDA vesicles depend upon disruption of the
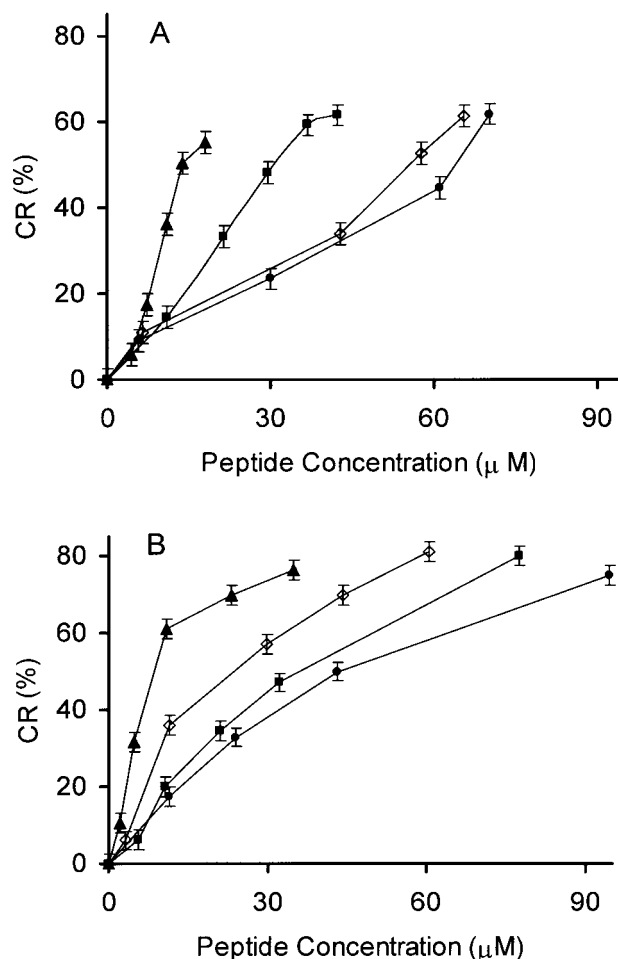

Figure 5   Colorimetric data obtained using lipid/PDA vesicles

Interface perturbation and more pronounced peptide–vesicle interactions are apparent when LPS is present in the bilayer. Graphs show the relationship between the colorimetric response (%CR) induced by different concentrations of bound peptides in aqueous solutions containing (**A**) DMPG/DMPC/PDA or (**B**) LPS/DMPC/PDA vesicles. Peptides examined: ■, PMB; ●, PMBN; ◇, Ala$_6$-PMBN; ▲, dPMBN.

lipid interface by membrane-interacting compounds and by their depth of penetration into the lipid layer [16,17]. In particular, we observed a correlation between the relative effect of the membrane-active compounds upon the lipid surface and the degree of colour change [16–18,21]. Peptides that preferably disrupt the lipid head-group region were shown to induce more pronounced colour transitions, while deeper penetration into the hydrophobic lipid core generally gave rise to more moderate blue-to-red transformations [15]. This correlation has been ascribed to the perturbation of the pendant side chains of the PDA framework induced by the interfacial effect within the lipid domains transitions [24,28]. Thus greater lipid surface interactions would result in more pronounced perturbations of the adjacent polymer domains, giving rise to higher colorimetric response (%CR).

Figure 5 shows the quantitative relationships between the colorimetric transitions and concentrations of the PMB derivatives added to DMPG/DMPC/PDA vesicles (Figure 5A) and LPS/DMPC/PDA vesicles (Figure 5B). The compositions of these lipid/PDA models were selected in order to examine the effects of lipid type on membrane interactions of the peptides. Accurate interpretation of the colorimetric data requires calculations of the colour transitions induced only by *vesicle-bound* peptides, rather

than the *total* peptide concentration (which also includes unbound peptide in the aqueous solution [16,18]). Thus the curves shown in Figure 5 take into account the relative partition coefficients of the peptides with the lipid/PDA vesicles, calculated using the centrifugation binding assay described above (Figure 4 and Table 2). The colorimetric curves shown in Figure 5 exhibit an initial increase in %CR, and reach %CR values between 60% and 80%, corresponding to maximal red colour induced by the bound peptides. In general, the informative part of the colorimetric curves constitutes the slopes prior to saturation [15,16].

Examination of Figure 5 reveals both similarities as well as distinct differences in membrane interactions of the peptides. In both vesicle models the steepest colorimetric response (%CR) curve (i.e. greater blue-to-red transitions in relation to peptide concentration) is observed for dPMBN, for which 60% CR is attained after addition of less than 15 μM peptide concentration (Figures 5A and 5B). We have previously demonstrated that a relatively steep increase in %CR versus concentration is indicative of a pronounced perturbation of the lipid head-group region [16]. Accordingly, the colorimetric data suggest that dPMBN mostly binds at the lipid/water interface rather than penetrate into the hydrophobic core of the lipid bilayer. In comparison with dPMBN, which resides at the lipid surface, PMBN and Ala$_6$-PMBN both induce less %CR (on a peptide concentration basis), indicating deeper penetration into the lipid domains (Figures 5A and 5B). However, a difference appears between the behaviour of PMBN and Ala$_6$-PMBN in the two vesicle compositions. Specifically, in DMPG/DMPC/PDA vesicles, the %CR curves of the two analogues are almost coincident (Figure 5A), whereas, in the LPS/DMPC/PDA assembly, Ala$_6$-PMBN induces higher %CR than PMBN (Figure 5B). This result suggests greater interfacial interaction for Ala$_6$-PMBN.

The colorimetric analysis further points to the specific role of LPS in eliciting surface interaction of the PMBN analogues (Figure 5B). For all three peptides the presence of LPS within the lipid bilayers increases the %CR induced by the peptide. For example, dPMBN at 15 μM gave rise to %CR of 50% in DMPG/DMPC/PDA vesicles, but induced above 65% in the LPS/DMPC/PDA system, and the corresponding values for PMBN were about 15 and 25% respectively. Ala$_6$-PMBN exhibited a particularly significant difference in its behaviour in the two compositions: less than 20% %CR induced in DMPG/DMPC/PDA vesicles and about around 45% in the LPS/DMPC/PDA assembly. This is further indication for the preferred surface localization of Ala$_6$-PMBN in LPS-containing bilayers.

Interestingly, PMB induces a moderate increase of %CR in the DMPG/DMPC/PDA vesicles, with the %CR dose–response curve appearing between the dPMBN curve on the one hand and PMBN Ala$_6$-PMBN on the other (Figure 5A). This result suggests that PMB perturbs both the head-group region and inner core of the lipid assembly. The effect of LPS in promoting penetration of PMB into the bilayer is also clearly apparent in Figure 5(B), which shows that lower %CR values are induced by the parent peptide in the LPS/DMPC/PDA system.

Fluorescence and ESR spectroscopic analyses

Application of fluorescence quenching spectroscopy and ESR complements the colorimetric measurements and provides additional information on the interactions of the peptides with the biomimetic lipid/PDA assemblies. Figure 6 depicts time–decay curves of the NBD-PE fluorescence probe embedded within DMPG/DMPC/PDA and LPS/DMPC/PDA vesicles respectively after addition of the fluorescence quencher sodium dithionite [33–35]. The fluorescence marker in NBD-PE is localized closer to the
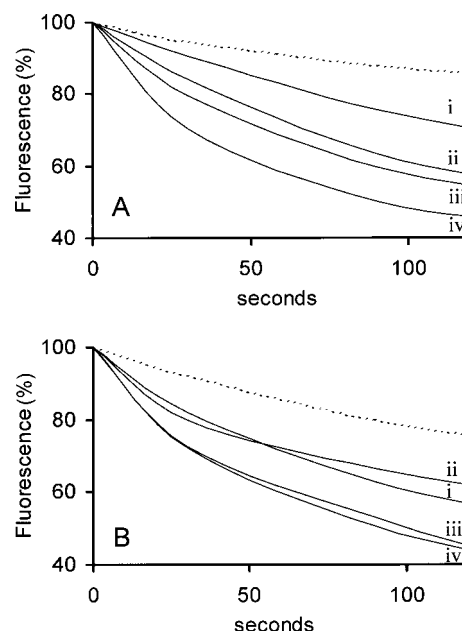

Figure 6   Fluorescence quenching of NBD-PE incorporated within lipid/PDA vesicles

Different extents of lipid-interface perturbation by PMBN analogues are shown, the greatest effect being induced by dPMBN. Time–decay curves of the fluorescence emission of NBD-PE (at 535 nm) were recorded following the addition of peptides to vesicles containing (**A**) NBD-PE/DMPG/DMPC/PDA (molar ratio 0.02:1:1:3) or (**B**) NBD-PE/LPS/DMPC/PDA (0.02:0.1:2:3). Broken curves indicate control vesicles (no peptide added). Analogues added: i, PMB; ii, PMBN; iii, Ala$_6$-PMBN; iv, dPMBN.

head-group region of the lipid bilayer and thus is a sensitive probe for interfacial perturbations by membrane-active species [34].

Figure 6 demonstrates that, in both biomimetic vesicle systems, all three PMBN analogues induced faster quenching of the NBD fluorescence, resulting from their interactions with the lipid moieties. Differences are apparent, however, among the peptides. dPMBN, for example, gave rise to the highest quenching among the analogues, both in DMPG/DMPC/PDA vesicles (less than 50% fluorescence observed after 2 min; Figure 6A) and LPS/DMPC/PDA vesicles (around 45% signal at 2 min; Figure 6B). This result is indicative of the pronounced association of the peptide at the lipid/water interface, which allows the soluble dithionite easier access to the NBD moieties located closer to the lipid bilayer surface. This interpretation is fully consistent with the colorimetric data discussed above (Figure 5).

Slower fluorescence quenching was recorded for PMBN and Ala$_6$-PMBN, albeit differences are observed between the two vesicle systems. PMBN gave rise to a relatively slow quenching: -60% signal after 120 s in NBD-PE/DMPG/DMPC/PDA and 70% in NBD-PE/LPS/DMPC/PDA vesicles (curve ii, Figure 6), consistent with the lesser head-group disruption by this peptide inferred from the colorimetric analysis (Figure 5). Similarly, Ala$_6$-PMBN induced stronger quenching in the NBD-PE/LPS/DMPC/PDA vesicle system (curve iii, Figure 6B), explained by the more pronounced interfacial association of this analogue in the LPS-containing bilayers.

The quenching rate of the parent peptide PMB was the slowest among the peptides examined in the two vesicle systems (curve i, Figure 6). This result might correspond to a lesser interfacial localization of PMB compared with its analogues. Deeper penetration of PMB into the bilayer in the LPS-containing vesicles was also inferred from the colorimetric analysis (Figure 5

Peptide	Vesicle composition . . .	A'_{zz} (mT)	
		DMPG/DMPC/PDA	LPS/DMPC/PDA
None (control)		4.81	4.75
PMBN		5.14	5.38
Ala$_6$-PMBN		5.30	5.53
dPMBN		5.57	5.49

above). The slowest quenching rate induced by PMB in the NBD-PE/DMPG/DMPC/PDA vesicles (curve i, Figure 6A), however, seems different from the colorimetric measurements in DMPG/DMPC/PDA vesicles (Figure 5A), which indicated intermediate penetration of the peptide into the DMPG/DMPC bilayer. This discrepancy could be related to the different biophysical parameters measured in the two experimental approaches – bilayer disruption in the colorimetric analysis compared with fluorescence decay of a surface-incorporated fluorescent probe in the quenching experiment.

ESR data, acquired using phospholipid/PDA vesicles incorporating stearic acid to which the doxyl spin label is covalently attached in carbon position 5 in the acyl chain (denoted 5-DS), illuminate the dynamic effects of peptide binding on to the lipid moieties within the lipid/PDA vesicles (Table 3). Spin-labelled lipid probes have been extensively used as a tool for probing the organization and local motion within lipid membranes [36,37]. The lipid/spin-label molar ratio of 100:1 employed in the experiments described here does not alter the properties and organization of the phospholipid/PDA vesicles. In particular, the colorimetric transformations of the vesicles were not affected by addition of the spin label [15].

Table 3 outlines the values of the parallel hyperfine splitting parameter, $2A'_{zz}$, obtained from the ESR spectra of 5-DS labels incorporated within the two lipid-vesicle models after the addition of the different PMBN analogues. It is generally recognized that the $2A'_{zz}$ parameter reflects the spin-label dynamics within the slow-motion region [36]. The ESR results in Table 3 indicate that the PMB derivatives modify the dynamic properties of the lipid moieties. In all samples the peptides gave rise to significantly higher $2A'_{zz}$ values of the doxyl label – corresponding to greater rigidity of the lipid domains surrounding the spin label [36]. Importantly, these changes in the $2A'_{zz}$ splitting of 5-DS seem to parallel the colorimetric transitions induced by the peptides (Figure 5) and the fluorescence-quenching data (Figure 6). dPMBN, for example, induces pronounced stiffening of the lipid assembly both in DMPG/DMPC/PDA vesicles ($2A'_{zz} = 5.49$ mT) and in LPS/DMPC/PDA vesicles ($2A'_{zz} = 5.57$ mT; Table 3). These data are consistent with the binding of dPMBN at the lipid/water interface, because the spin label in 5-DS is adjacent to the lipid head-group region. The ESR results recorded for Ala$_6$-PMBN also corroborate the colorimetric and fluorescence data. Specifically, the higher $2A'_{zz}$ value of 5.53 mT induced after the addition of the peptide to LPS/DMPC/PDA vesicles compared with a $2A'_{zz}$ value of 5.30 mT in DMPG/DMPC/PDA vesicles indicates a stronger interfacial binding when LPS is present in the bilayer. PMBN gives rise to moderate increases in the $2A'_{zz}$ values in both vesicle systems (5.14 and 5.38 mT in DMPG/DMPC/PDA and LPS/DMPC/PDA vesicles respectively; Table 2), suggesting deeper penetration into the lipid bilayer.

DISCUSSION

The present study analysed structural aspects of membrane binding and lipid interactions of PMB and its derivatives. The colorimetric assay facilitated comparisons between the effects of ring modification (in the case of PMBN and dPMBN) and side-chain substitution (Ala$_6$-PMBN) on the association and penetration of the peptides to a biomimetic lipid/polymer assembly. The results point to distinct parameters affecting the biological activities of the PMBN analogues.

The binding data in Figures 3 and 4 clearly demonstrated that the presence of LPS within lipid assemblies promotes higher peptide affinities and more pronounced interactions of the peptides at the lipid/water interface. The colorimetric and spectroscopic analyses further indicate that LPS not only induces stronger binding of the peptide analogues to the vesicles, but also elicits specific surface interactions. This interpretation is based upon the steeper rises in %CR versus peptide concentrations depicted in Figure 5, as well as the faster fluorescence quenching (Figure 6) and greater rigidity of the lipid bilayer (Table 3).

The experiments illuminate the possible functional roles of the cyclic ring and hydrophobic terminal residue of PMB. The colorimetric data suggest that the cyclic ring not only has a distinct role in peptide attachment to the membrane interface, but also affects the degree of penetration into the lipid assembly. In that regard, the comparison between lipid interaction and relative penetration of PMBN and dPMBN, which differ only in the chirality of ring residues, yielded important information. dPMBN strongly interacts with the lipid head-group region and does not insert deeply into the membrane – inferred both from the affinity measurements (Figures 3 and 4) as well as the colorimetric and spectroscopic data (Figures 5 and 6). The predominant interface association of dPMBN most likely explains the significantly decreased biological action of the peptide [13].

Distinct behaviour was observed for PMBN. The colorimetric and spectroscopic data suggest that PMBN undergoes deeper insertion into the lipid layer, regardless of whether DMPG or LPS are present within the lipid assembly. This result is quite intriguing, particularly in the light of the absence of the hydrophobic residue in PMBN, and might point to the significance of the cyclic ring for directing the peptide into the alkyl core of the lipid bilayer. Importantly, the insertion of PMBN is consistent with the presence of the hydrophobic segment D-Phe-Leu in the ring, which has recently been shown to serve as an important recognition factor [38]. This conclusion further explains the similar binding properties of dPMBN and PMBN, but the almost complete biological inactivation of dPMBN [13]. In addition to the essential functional role of the PMBN ring, the data testified to an involvement of the mildly hydrophobic Ala$_6$ peptidic side chain in lipid interactions, particularly in binding at the lipid/water interface. Owing to its long lipophilic peptide residue, Ala$_6$-PMBN was expected to penetrate relatively deeply into the lipid core. However, significant interfacial perturbation rather than penetration was detected when LPS was present within the lipid assembly (Figures 5 and 6 and Table 3). The effect of Ala$_6$-PMBN on the head-group region of LPS/DMPC/PDA appeared even stronger than PMBN. This result attests to the fact that the side chain, and not only the cyclic moiety, contributes to interactions with the LPS head-group and participates in molecular rearrangement closer to the lipid/water interface.

The experiments seem to underscore important molecular aspects pertaining to outer-membrane permeation and lytic activity of PMB. The colorimetric assay indicates that the parent peptide induces perturbation both at the lipid/water interface as well as deeper within the hydrophobic interior of the membrane.

The experimental observations indeed suggest that the potent biological effects of PMB, specifically its membrane- permeation properties and high toxicity, are related to its ability to disrupt both lipid head-groups as well as the hydrophobic domains of the membrane. This interpretation could also explain the generally lower permeation and reduced lytic activities of the molecules derived from PMB; alteration of either the ring or the terminal acyl residue might interfere with the capabilities of the peptide to penetrate and disrupt cellular membranes.

The experiments presented here could underscore distinct molecular aspects pertaining to outer membrane permeation and lytic activities of PMB and its derivatives. The biomimetic lipid/PDA vesicle assay demonstrated that the peptides induced perturbations both at the lipid/water interface as well as deeper within the hydrophobic interior of the membrane. Furthermore, the present study indicates that attachment to the lipid bilayer, and the degree of penetration into the lipid bilayer, are two distinct events in membrane interactions of the peptides.

REFERENCES

1 Nikaido, H. and Vaara, M. (1987) Outer membrane. In *Escherichia coli* and *Salmonella typhimurium* (Neidhardt, F. C., ed.), pp. 7–22, American Society for Microbiology, Washington, DC

2 Cronan, J. E., Gennis, R. B. and Maloy, S. M. (1987) Cytoplasmic Membrane. In *Escherichia coli* and *Salmonella typhimurium* (Neidhardt, F. C., ed.), pp. 31–55, American Society for Microbiology, Washington, DC

3 Brandenburg, K., Kusumoto, S. and Seydel, U. (1997) Conformational studies of synthetic lipid A analogs and partial structures by infrared spectroscopy. Biochem. Biophys. Acta **1329**, 183–201

4 Snyder, S., Kim, D. and McIntosh T. J. (1999) Lipopolysaccharide bilayer structure: effect of chemotype, core mutations, divalent cations, and temperature. Biochemistry **38**, 10758–10767

5 Danner, R. L., Joiner, K. A., Rubin M., Patterson, W. H., Johnson, N., Ayers, K. M. and Parrillo, J. E. (1989) Purification, toxicity, and antiendotoxin activity of polymyxin B nonapeptide. Antimicrob. Agents Chemother. **33**, 1428–1434

6 Moore, R. A., Bates, N. C. and Hancock, R. E. (1986) Interaction of polycationic antibiotics with *Pseudomonas aeruginosa* lipopolysaccharide and lipid A studied by using dansyl-polymyxin. Antimicrob. Agents Chemother. **9**, 496–500

7 Chihara, S., Ito, A., Yahata, M., Tobita, T. and Koyama, Y. (1973) Colistin nonapeptide derivatives. I. Chemical synthesis and characterization of α-N-octanoyl and other α-N-acyl colistin nonapeptide derivatives. Agric. Biol. Chem. **37**, 2709

8 Chihara, S., Ito, A., Yahata, M., Tobita, T. and Koyama, Y. (1974) Colistin nonapeptide derivatives. II. Chemical synthesis, isolation, and characterization of α-N-fattyacyl colistin nonapeptide with special reference to the correlation between antimicrobial activity and carbon number of fattyacyl moiety. Agric. Biol. Chem. **38**, 521–529

9 Duwe, A. K., Rupar, C. A., Horsman, G. B. and Vas, S. I. (1986) *In vitro* cytotoxicity and antibiotic activity of polymyxin B nonapeptide. Antimicrob. Agents Chemother. **30**, 340–341

10 Chihara, S., Ito, A., Yahata, M., Tobita, T. and Koyama, Y. (1973) Enzymatic degradation of colistin. Isolation and identification of α-N-acyl α,γ-diaminobutyric acid and colistin nonapeptide. Agric. Biol. Chem. **37**, 2455–2463

11 Vaara, M. and Vaara, T. (1983) Sensitization of Gram-negative bacteria to antibiotics and complement by a nontoxic oligopeptide. Nature (London) **303**, 526–528

12 Tsubery, H., Ofek, I., Cohen, S. and Fridkin, M. (2000) Structure–function studies of polymyxin B nonapeptide: implications to sensitization of gram-negative bacteria. J. Med. Chem. **43**, 3085–3092

13 Tsubery, H., Ofek, I., Cohen, S. and Fridkin, M. (2000) The functional association of polymyxin B with bacterial lipopolysaccharide is stereospecific: studies on polymyxin B nonapeptide. Biochemistry **39**, 11837–11844

14 Tsubery, H., Ofek, I., Cohen, S. and Fridkin, M. (2001) N-terminal modifications of polymyxin B nonapeptide and their effect on antibacterial activity. Peptides **22**, 1675–1681

15 Kolusheva, S., Shahal, T. and Jelinek, R. (2000) Peptide–membrane interactions studied by a new phospholipid/polydiacetylene colorimetric vesicle assay. Biochemistry **39**, 15851–15859

16 Kolusheva, S., Boyer, L. and Jelinek, R. (2000) A colorimetric assay for rapid screening of antimicrobial peptides. Nat. Biotechnol. **18**, 225–227

17 Kolusheva, S., Kafri, R., Katz, M. and Jelinek, R. (2001) Rapid colorimetric detection of antibody–epitope recognition at a biomimetic membrane interface. J. Am. Chem. Soc. **123**, 417–422

18 Evrard, D., Touitou, E., Kolusheva, S., Fishov, Y. and Jelinek, R. (2001) A new colorimetric assay for studying and rapid screening of membrane penetration enhancers. Pharm. Res. **18**, 943–949

19 Gaboriaud, F., Golan, R., Volinsky, R., Berman, A. and Jelinek, R. (2001) Organization and structural properties of Langmuir films composed of conjugated polydiacetylene and phospholipids. Langmuir **17**, 3651–3657

20 Volinsky, R., Gaboriaud, F., Berman, A. and Jelinek R. (2002) Morphology and organization of phospholipid/diacetylene Langmuir films studied by Brewster angle microscopy and fluorescence microscopy. J. Phys. Chem. **106**, 9231–9236

21 Kolusheva, S., Wachtel, E. and Jelinek, R. (2003) Biomimetic lipid/polymer colorimetric membranes: molecular and cooperative properties. J. Lipid Res. **44**, 65–71

22 Satchell, D. P., Sheynis, T., Shirafuji, Y., Kolusheva, S., Ouellette, A. and Jelinek, R. (2003) Interactions of mouse paneth cell α-defensins with membranes studied by a biomimetic lipid/polymer colorimetric assay. J. Biol. Chem. **278**, 13838–13847

23 Lowry, O. H., Rosebrough, N. J., Farr, A. L. and Randall, R. J. (1951) Protein measurement with the Folin phenol reagent. J. Biol. Chem. **193**, 265–275

24 Okada, S., Peng, S., Spevak, W. and Charych, D. (1998) Color and chromism of polydiacetylene vesicles. Acc. Chem. Res. **31**, 229–239

25 Vaara, M. and Viljanen, P. (1985) Binding of polymyxin B nonapeptide to Gram-negative Bacteria. Antimicrob. Agents Chemother. **27**, 548–554

26 Ofek, I., Cohen, S., Rahmani, R., Kabha, K., Tamarkin, D., Herzig, Y. and Rubinstein, E. (1994) Antibacterial synergism of polymyxin B nonapeptide and hydrophobic antibiotics in experimental gram-negative infections in mice. Antimicrob. Agents Chemother. **38**, 374–377

27 Li, C., Budge, L. P., Driscoll, C. D., Willardson, B. M., Allman, G. W. and Savage, P. B. (1999) Incremental conversion of outer-membrane permeabilizers into potent antibiotics for Gram-negative Bacteria. J. Am. Chem. Soc. **121**, 931–940

28 Ringsdorf, H., Schlarb, B. and Venzmer, J. (1988) Molecular architecture and function of polymeric oriented systems: models for the study of organization, surface recognition, and dynamics of biomembranes. Angew. Chem. Int. Edn. Engl. **27**, 113–158

29 Charych, D. H., Nagy, J. O., Spevak, W. and Bednarsky, M. D. (1993) Direct colorimetric detection of a receptor–ligand interaction by a polymerized bilayer assembly. Science **261**, 585–588

30 Latorre, R. and Alvarez, O. (1981) Voltage-dependent channels in planar lipid bilayer membranes. Physiol. Rev. **61**, 77–150

31 Fidai, S., Farmer, S. W. and Hancock, R. E. W. (1997) Interaction of cationic peptides with bacterial membranes. Methods Mol. Biol. **78**, 187–204

32 Oren, Z. and Shai, Y. (1997) Selective lysis of bacteria but not mammalian cells by diastereomers of melittin: structure–function study. Biochemistry **36**, 1826–1835

33 Chattopadhyay, A. and London, E. (1987) Parallax method for direct measurement of membrane penetration depth utilizing fluorescence quenching by spin-labeled phospholipids. Biochemistry **26**, 39–45

34 McIntyre, J. C. and Sleight, R. G. (1991) Fluorescence assay for phospholipid membrane asymmetry. Biochemistry **30**, 11819–11827

35 Yu, B.-Z., Ghomashchi, F., Cajal, Y., Annand, R. R., Berg, O. G., Gelb, M. H. and Jain, M. K. (1997) Use of an imperfect neutral diluent and outer vesicle layer scooting mode hydrolysis to analyze the interfacial kinetics, inhibition, and substrate preferences of bee venom phospholipase A_2. Biochemistry **36**, 3870–3881

36 Marsh, D. (1981) Membrane Spectroscopy, Springer-Verlag, Berlin

37 Kleinschmidt, J. H., Mahaney, J. E., Thomas, D. D. and Marsh, D. (1997) Interaction of bee venom melittin with zwitterionic and negatively charged phospholipid bilayers: a spin-label electron spin resonance study. Biophys. J. **72**, 767–778

38 Tsubery, H., Ofek, I., Cohen, S., Eisenstein, M. and Fridkin, M. (2002) Modulation of the hydrophobic domain of polymyxin B nonapeptide: effect on outer-membrane permeabilization and lipopolysaccharide neutralization. Mol. Pharm. **62**, 1036–1042